

PAPER • OPEN ACCESS

Novel emergent phases in a two-dimensional superconductor

To cite this article: Simrandeep Kaur *et al* 2024 *New J. Phys.* **26** 083001

View the [article online](#) for updates and enhancements.

You may also like

- [Direct real photons in relativistic heavy ion collisions](#)
Gabor David

- [From non-interacting to interacting picture of thermodynamics and transport coefficients for quark gluon plasma](#)
Sarthak Satapathy, Souvik Paul, Ankit Anand et al.

- [Soliton solutions of MHD equations in cold quark gluon plasma](#)
Azam Ghaani and Kurosh Javidan

New Journal of Physics

The open access journal at the forefront of physics

Deutsche Physikalische Gesellschaft 

IOP Institute of Physics

Published in partnership
with: Deutsche Physikalische
Gesellschaft and the Institute
of Physics



PAPER

OPEN ACCESS

RECEIVED
18 March 2024

REVISED
25 July 2024

ACCEPTED FOR PUBLICATION
26 July 2024

PUBLISHED
5 August 2024

Original Content from
this work may be used
under the terms of the
[Creative Commons
Attribution 4.0 licence](#).

Any further distribution
of this work must
maintain attribution to
the author(s) and the title
of the work, journal
citation and DOI.



Novel emergent phases in a two-dimensional superconductor

Simrandeep Kaur¹, Hemanta Kumar Kundu², Sumit Kumar^{3,4}, Anjana Dogra^{3,4} , Rajesh Narayanan⁵, Thomas Vojta⁶ and Aveek Bid^{1,*} 

¹ Department of Physics, Indian Institute of Science, Bangalore 560012, India

² Braun Center for Sub-Micron Research, Department of Condensed Matter Physics, Weizmann Institute of Science, Rehovot 76100, Israel

³ CSIR-National Physical Laboratory, Dr K. S. Krishnan Road, New Delhi 110012, India

⁴ Academy of Scientific and Innovative Research (AcSIR), Ghaziabad, Uttar Pradesh 201002, India

⁵ Department of Physics, Indian Institute of Technology Madras, Chennai 600036, India

⁶ Department of Physics, Missouri University of Science and Technology, Rolla, MO 65409, United States of America

* Author to whom any correspondence should be addressed.

E-mail: aveek@iisc.ac.in

Keywords: superconductor, Griffiths singularity, anomalous metal, Oxide heterostructure

Supplementary material for this article is available [online](#)

Abstract

In this letter, we report our observation of an extraordinarily rich phase diagram of a LaScO₃/SrTiO₃ heterostructure. Close to the superconducting transition temperature, the system hosts a superconducting critical point of the Infinite-randomness type characterized by an effective dynamical exponent νz that diverges logarithmically. At lower temperatures, we find the emergence of a magnetic field-tuned metallic phase that co-exists with a quantum Griffiths phase (QGP). Our study reveals a previously unobserved phenomenon in 2D superconductors—an unanticipated suppression of the QGP below a crossover temperature in this system. This concealment is accompanied by the destruction of the superconducting quantum critical point (QCP) signaled by a power-law divergence (in temperature) of the effective dynamical exponent. These observations are entirely at odds with the predictions of the infinite-randomness scenario and challenge the very concept of a vanishing energy scale associated with a QCP. We develop and discuss possible scenarios like smearing of the phase transition that could plausibly explain our observations. Our findings challenge the notion that QGP is the ultimate ground state in two-dimensional superconductors.

The study of two-dimensional (2D) superconductors has emerged as a frontier in condensed matter physics, offering a fascinating window into the interplay of quantum mechanics and material science [1, 2]. The interest in 2D superconductors extends beyond the quantum phenomenon they host; their inherently thin nature and surface accessibility allow for unprecedented tunability through external stimuli, such as pressure, magnetic fields, and electrostatic gating. This tunability paves the way for a deeper understanding of superconductivity and holds the promise of novel technological applications, including quantum computing [3, 4] and ultra-sensitive detectors [5]. Recently, the exploration of 2D superconductors has received an impetus fueled by the advent of sophisticated material synthesis and characterization techniques enabling the creation and detailed study of these materials with unprecedented precision.

These systems are a repository of exciting phases. The principal among these is the quantum Griffiths phase (QGP) [6–17]. The QGP arises due to the formation of disorder-induced rare superconducting puddles embedded in the insulating bulk and their slow dynamics caused by coupling to the dissipative metallic environment. The associated fluctuations influence the entire system's behavior, leading to unconventional scaling properties and novel critical behavior. The QGP is predicted to be concomitant with the unconventional quantum critical behavior governed by an infinite-randomness critical point (IRCP) [18]. At an IRCP, the dynamical critical behavior is not of the conventional power-law type but instead is activated, with a dynamical critical exponent z that diverges as one approaches the quantum phase transition [19–21].

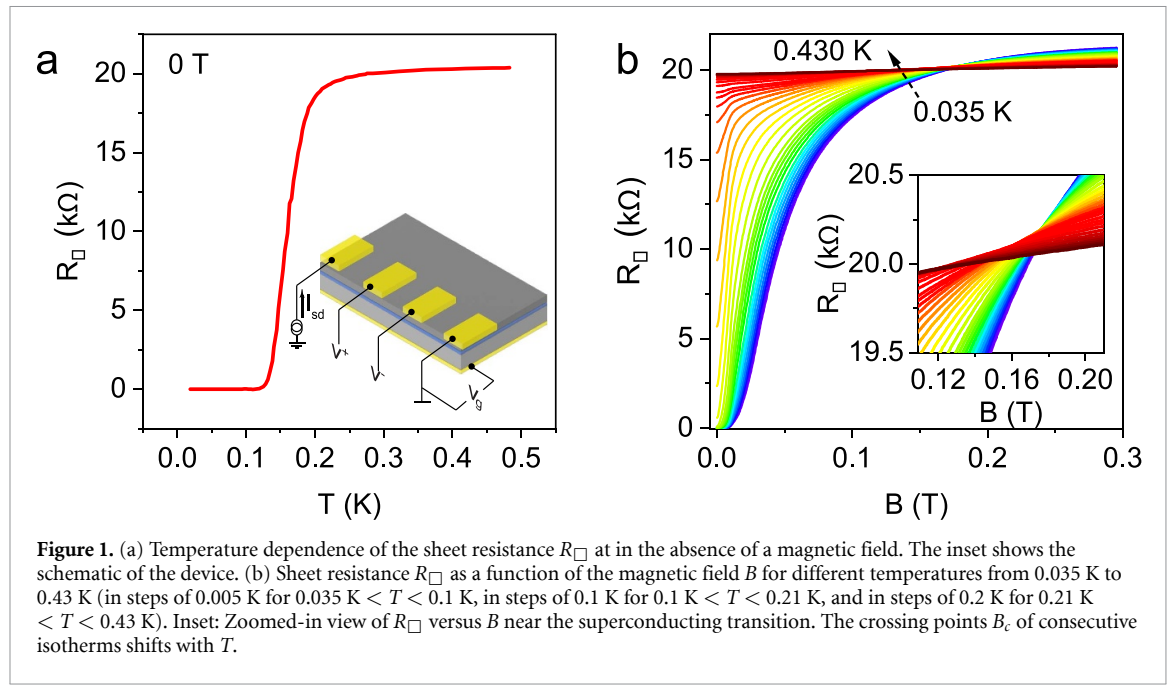


Figure 1. (a) Temperature dependence of the sheet resistance R_{\square} at in the absence of a magnetic field. The inset shows the schematic of the device. (b) Sheet resistance R_{\square} as a function of the magnetic field B for different temperatures from 0.035 K to 0.43 K (in steps of 0.005 K for $0.035 \text{ K} < T < 0.1 \text{ K}$, in steps of 0.1 K for $0.1 \text{ K} < T < 0.21 \text{ K}$, and in steps of 0.2 K for $0.21 \text{ K} < T < 0.43 \text{ K}$). Inset: Zoomed-in view of R_{\square} versus B near the superconducting transition. The crossing points B_c of consecutive isotherms shifts with T .

Per conventional wisdom, [22, 23], the quantum ground states of these systems are either superconducting or insulating. This implies a direct quantum phase transition between these competing ground state phases accessed by tuning non-thermal parameters such as disorder, magnetic field, or carrier density. However, a welter of experimental evidence points to the existence of a broad intermediate weakly metallic regime intervening in the superconducting and insulating phases in several 2D disordered superconductors [24–27]. The effect of the presence of this dissipative environment proximate to the superconducting quantum critical point (QCP) on the scaling behavior of the system remains ill-explored [28].

In this letter, we address these open questions. Using the scaling of magnetoresistivity data, we show that the quasi-2D electron gas (q-2DEG) at the interface of $\text{LaScO}_3/\text{SrTiO}_3$ heterostructures has a very unusual phase diagram. Consistent with theoretical predictions on the existence of an IRCP [13, 14, 19–21], the dynamical exponent $z\nu$ diverges logarithmically with decreasing temperature, indicating the existence of a QGP. Most crucially, below a crossover temperature T^* , we encounter a novel region of the phase diagram where the QGP gets strongly suppressed in conjunction with the smearing of the superconducting QCP. This low-temperature suppression of the Griffiths phase signaled via a power-law divergence of the effective temperature dependent dynamical exponent with decreasing temperature is incompatible with the notion of a vanishing energy scale associated with a QCP. This novel effect, which, to our knowledge, has not been experimentally observed, is one of the central aspects of our results. We elucidate possible mechanisms for this exciting new phenomenon and its implications on quantum phase transitions. Our combination of quantum transport measurements and state-of-the-art scaling analysis indicates that, contrary to conventional wisdom, the QGP may not be the ultimate ground state in disordered 2D superconductors.

Our measurements were performed on 10-unit cell thick films of LaScO_3 epitaxially grown on (001) TiO_2 terminated SrTiO_3 single-crystal substrates. The interface hosts a q-2DEG [29]. Electrical contacts were made with Al wire using an ultrasonic wire bonder that breaks the 10-unit cells of LaScO_3 and makes ohmic contact with the underlying q-2DEG [30]. A gold film deposited at the back of the STO acts as the back-gate electrode to tune the number density at the interface, with STO serving as the gate dielectric (figure 1(a) inset). The transport measurements were carried out in a cryogen-free dilution refrigerator with a base temperature of 20 mK. Figure 1(a) shows the T -dependence of the sheet resistance R_{\square} at a prototypical gate voltage of $V_g = 100 \text{ V}$. The q-2DEG undergoes a superconducting transition $T_c^{\text{zero}} = 150 \text{ mK}$ —this is the first observation of superconductivity in this particular oxide heterostructure. We identify T_c^{zero} operationally as the temperature where resistance is 1% of the normal state resistance.

In figure 1(b), we analyze the magnetoresistance isotherms $R_{\square}(B)$ over a temperature range $0.035 \text{ K} < T < 0.430 \text{ K}$. For a typical quantum phase transition from a superconductor to an insulator phase, the magnetoresistance isotherms cross at a single critical point [31, 32]. However, a zoom-in of the data (inset of figure 1(b)) shows that this is not the case here; the crossing points $B_c(T)$ between successive isotherms drift with changing temperature. Such unconventional behavior of the magnetoresistance is a

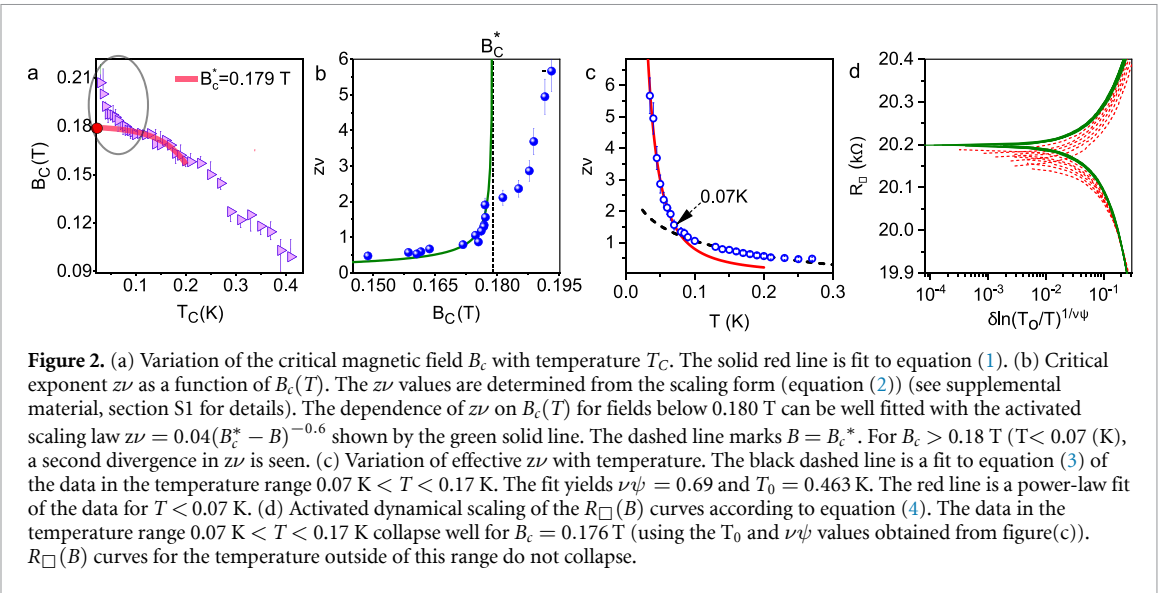


Figure 2. (a) Variation of the critical magnetic field B_c with temperature T_C . The solid red line is fit to equation (1). (b) Critical exponent $z\nu$ as a function of $B_c(T)$. The $z\nu$ values are determined from the scaling form (equation (2)) (see supplemental material, section S1 for details). The dependence of $z\nu$ on $B_c(T)$ for fields below 0.180 T can be well fitted with the activated scaling law $z\nu = 0.04(B_c^* - B)^{-0.6}$ shown by the green solid line. The dashed line marks $B = B_c^*$. For $B_c > 0.18$ T ($T < 0.07$ K), a second divergence in $z\nu$ is seen. (c) Variation of effective $z\nu$ with temperature. The black dashed line is a fit to equation (3) of the data in the temperature range $0.07 \text{ K} < T < 0.17$ K. The fit yields $\nu\psi = 0.69$ and $T_0 = 0.463$ K. The red line is a power-law fit of the data for $T < 0.07$ K. (d) Activated dynamical scaling of the $R_\square(B)$ curves according to equation (4). The data in the temperature range $0.07 \text{ K} < T < 0.17$ K collapse well for $B_c = 0.176$ T (using the T_0 and $\nu\psi$ values obtained from figure(c)).

harbinger of the Infinite Randomness scenario and stems from sub-leading corrections to scaling arising from the leading irrelevant operator [7–10, 12, 17]. The locus in the $T - B$ plane of this set of crossing points coincides with that of points defined by $dR(B, T)/dT = 0$ [10] and determines the critical magnetic field (B_c) and temperature (T_c) for the onset of superconducting fluctuations. Superconducting quantum fluctuations are operative in the temperature window between T_c^{zero} and T_c . In line with expectations at a critical point, T_c marks the temperature where the fluctuations become scale invariant. This set of crossing points, that of neighboring isotherms that determine T_c , is used to construct figure 2(a). Furthermore, if the superconducting QCP is of the Infinite Randomness type, the shift of the crossing fields (figure 2(a)) is given by [12]:

$$\left(\frac{B_c^* - B_c(T)}{B_c^*} \right) = u \left(\ln \left(\frac{T_0}{T} \right) \right)^{-1/\nu\psi - \omega/\psi}. \quad (1)$$

Here, $\nu = 1.2$ for the correlation length critical exponent and $\psi = 1/2$ for the tunneling critical exponent, as predicted for the IRCP scenario in two-dimensions [33], u and ω are, respectively, the leading irrelevant operator and associated exponent responsible for the correction to the scaling. The solid red line in figure 2(a) is fit to equation (1). The fit yields $B_c^* = 0.179$ T. Interestingly, at low temperatures, the phase boundary deviates from the prediction of equation (1) (marked by an ellipse in figure 2(a)) and develops a tail at low temperatures.

To probe this deviation further, we perform a detailed analysis of the magnetoresistance data utilizing a power-law scaling ansatz valid in two dimensions: [34]:

$$R_\square(B) = R_c f \left[(B - B_c) \left(\frac{T_0}{T} \right)^{1/\nu z} \right]. \quad (2)$$

Here, R_c is the critical sheet resistance, and $f(x)$ is a scaling function with $f(0) = 1$. The value of the exponent combination $z\nu$ is obtained by applying equation (2) to the magnetoresistance data. (See supplemental material section S1) [7]. The resulting $z\nu$ values, presented in figure 2(b), demonstrate a fascinating T and B dependence: With decreasing temperature (and the corresponding increase in $B_c(T)$), $z\nu$ values sharply increase as one approaches the characteristic magnetic field B_c^* . For $T > 70$ mK ($B_c^* < 0.18$ T), $z\nu$ can be well fitted with a power-law of the form $z\nu \sim (B_c^* - B_c)^{-\nu\psi}$, and is typically reminiscent of its behavior in the QGP associated with an IRCP [7, 13, 14, 18]. The fit to the data gives $B_c^* = 0.179$ T. Now, very interestingly, upon further lowering the temperature (increasing $B_c(T)$), a kink-like feature develops, leading to a second sharp increase of $z\nu$. This observation of two distinct upturns in the temperature dependence of $z\nu(T)$ is unforeseen that all previous studies reported only a single upturn in the field-dependence of $z\nu(T)$ [7–12] and is the central result of this letter.

Further insight into the anomalous behavior of $z\nu$ can be obtained by studying its T -dependence, plotted in figure 2(c). For systems exhibiting a quantum phase transition of the infinite-randomness variety, the

effective $z\nu$ extracted using the power-law scaling ansatz (equation (2)) has a logarithmic T -dependence [12],

$$\left(\frac{1}{\nu z}\right)_{\text{eff}} = \frac{1}{\nu\psi} \frac{1}{\ln(T_0/T)} . \quad (3)$$

The data in figure 2(c) can be well fitted with equation (3) over the T -range $70 \text{ mK} < T < 170 \text{ mK}$. The fit yields $T_0 = 460 \text{ mK}$ and $\nu\psi = 0.69$, in excellent agreement with the predictions for the 2D IRCP universality class [33].

In contrast, the $z\nu$ data in the temperature range below 0.07 K show a much stronger power-law temperature dependence with $z\nu(T) \sim T^{-1.9}$. This power-law divergence of $z\nu(T)$ is incompatible with the notion of a QCP that implies the existence of an energy scale (encoded in the denominator of equation (2)) that vanishes as $T \rightarrow 0$. A power-law divergence of $\nu z(T)$ belies this expectation as the function $T^{1/\nu z(T)}$ remains finite in the $T \rightarrow 0$ limit, suggesting a non-vanishing energy scale even at the lowest temperatures (refer to supplementary material section S9 for a detailed derivation). Consequently, the data allude to a physical mechanism that destroys the infinite-randomness superconducting transition and as a consequence the cut off of the accompanying quantum Griffiths effects. Finally, similar suppression of the Griffiths effects has been recently reported in the iron-based superconductor $\text{FeSe}_{0.89}\text{S}_{0.11}$ [17].

The emergence of an IRCP over the temperature range $0.07 \text{ K} - 0.17 \text{ K}$ and its eventual suppression below 0.07 K is also brought to the fore in figure 2(d), which analyzes the magnetoresistance data according to the activated scaling ansatz [35]:

$$R_{\square} = R_c f \left[\frac{(B - B_c^*)}{B_c^*} \ln(T_0/T)^{1/\nu\psi} \right] . \quad (4)$$

The values of T_0 and $\nu\psi$ used for this analysis are taken from the fit of the data in figure 2(c) to equation (3). The curves in the temperature range $T > 70 \text{ mK}$ all collapse onto two branches for $B_c^* = 0.176 \text{ T}$, which agrees well with the critical value B_c^* found in figures 2(a) and (b). Data for $T < 70 \text{ mK}$, on the other hand, do not collapse onto the universal curves, which once again indicates the destruction of the IRCP and the suppression of the associated Griffiths effects. Furthermore, the high-temperature data (for $T > 170 \text{ mK}$) do not scale, marking the high-temperature limit of the quantum critical region controlled by the IRCP.

Reiterating our results in the context of the above discussion, we stress that for $T < 0.07 \text{ K}$, we have shown that the Griffiths phase associated with the IRCP is destroyed. This destruction is signaled by the effective exponent combination $z\nu$ diverging stronger than the expected logarithmic functional form that obtains at the Infinite Randomness fixed point. This stronger-than-logarithmic divergence also negates the possibility of two different Griffiths phases (namely, one above 0.07 K and one below $T = 0.07 \text{ K}$). Furthermore, the fact that at low temperatures, the shift of the crossing points as a function of temperature does not conform to equation (1) shows clearly once again that the IRCP is destroyed (figure 2(a)) and implies that the tail that develops at low temperatures owes its origin to physics that is not connected to the IRCP.

We now turn our attention to plausible scenarios that can lead to the suppression of the QGP at ultra-low temperatures and which are concomitant to the emergence of the tail in figure 2(a) at low temperatures (please see supplementary information, section S11 for a more detailed discussion). The quantum Griffiths singularities arise due to the interplay of disorder, order-parameter symmetry, and Ohmic Landau damping of the superconducting order-parameter fluctuations caused by the coupling to soft fermionic particle-hole excitations [13, 14]. Changes in the dissipative environment of the order parameter fluctuations destroy the Griffiths singularities. Such a mechanism has been proposed, for example, to destabilize the magnetic QGP in itinerant Heisenberg magnets where the interplay of the bare Landau damping and the long-range RKKY interactions between the rare-regions produce stronger sub-Ohmic dissipation [36, 37]. Superconducting fluctuations are known to be subject to a similar oscillatory long-range interaction [38], leading to a possibility that the dissipative environment felt by the superconducting puddles could be sub-Ohmic. This, in turn, implies that below a crossover temperature scale, the emergent sub-Ohmic dissipation could freeze (phase-lock) individual rare regions, leading to a smearing of the superconducting QCP.

Thus, the low-temperature tail seen in figures 2(a), and (c) is compatible with the smeared QCP scenario elucidated above [39–41], wherein the Griffiths phase is destabilized towards the inhomogeneously ordered state. We note that a very similar explanation has been invoked previously to explain the failure of the power-law scaling of the magnetoconductance data in MoGe films in the presence of a dissipative bath (see, for example, [28]), highlighting the importance of the damping in such systems.

Information on the possible influence of the damping mechanism is provided by the plots of temperature dependence of R_{\square} at different magnetic fields. Figure 3(a) shows the data measured at $V_g = 100 \text{ V}$. With increasing B , the low-temperature resistance tends to flatten to a T -independent value. This is in sharp

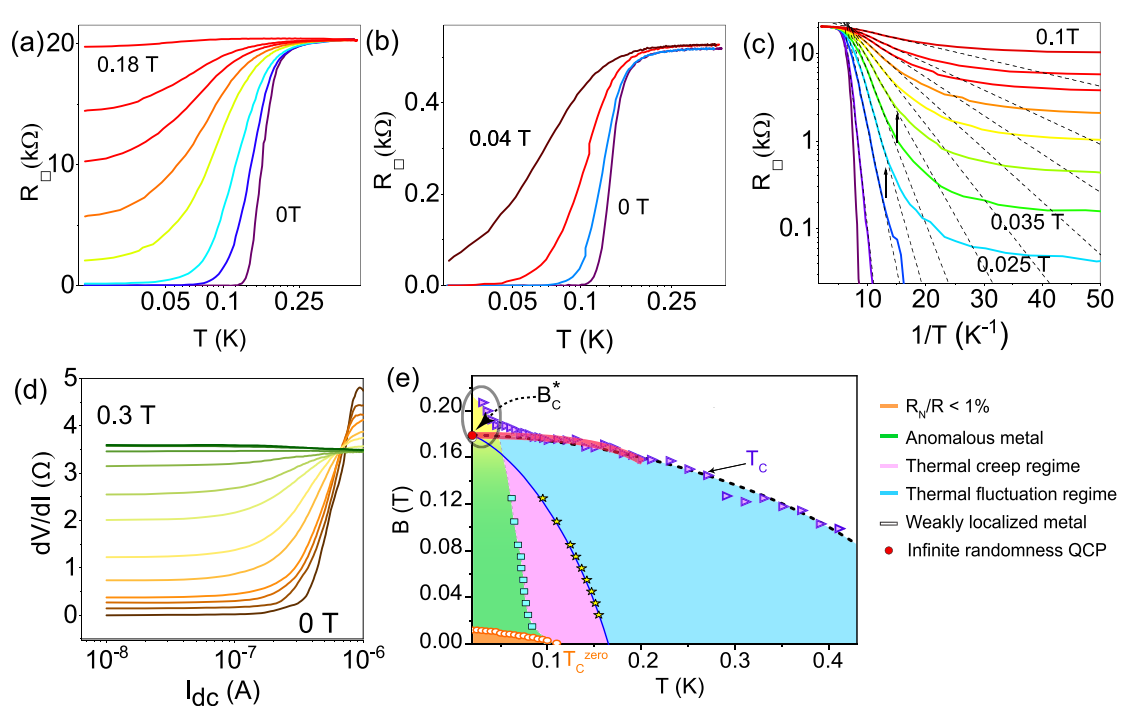


Figure 3. (a) Resistance versus temperature plot for $\text{LaScO}_3/\text{SrTiO}_3$ at a few representative values of B . The data were taken for $V_g = 100$ V. (b) Resistance versus temperature for $\text{LaAlO}_3/\text{SrTiO}_3$ heterostructure at different B . The resistance saturation seen for $\text{LaScO}_3/\text{SrTiO}_3$ is absent for this material. (c) Arrhenius plot of the sheet resistance as a function of the inverse of temperature. The dashed lines are fits to the TAFF equation (see text). Arrows correspond to the points where sheet resistance deviates from the TAFF equation and saturates at a finite value, marking the phase boundary between AM and TAFF region (d) Differential resistance as a function of DC bias for different out-of-plane magnetic field values for $\text{LaScO}_3/\text{SrTiO}_3$ taken at $T = 0.02$ K. (e) Phase diagram in the T - B plane at $V_g = 100$ V for $\text{LaScO}_3/\text{SrTiO}_3$. The open orange circles at low T and low B mark the phase boundary of the superconducting state. Blue open squares demarcate the crossover between the AM and the TAFF regimes. The crossover from the TAFF regime to the one dominated by thermal fluctuations of the order parameter amplitude is marked by yellow stars. Purple triangles denote the crossover line between the weakly localized metal and the thermal fluctuation regime. The red-bold line comes from the fit to equation (1). The low-temperature tail (marked by an ellipse) is attributed to the smearing of the putative superconducting QCP at B_c^* . Yellow shade marks the region where QGP is suppressed. (See text for further details.).

contrast to the data for a similar system – $\text{LaAlO}_3/\text{SrTiO}_3$ (LAO/STO) heterostructure, where such a saturation is absent (figure 3(b)). A $\log(R_\square) - 1/T$ plot for the LSO/STO device shows that upon lowering the temperature, the activated behavior of the resistance changes to a temperature-independent resistance (figure 3(c)). At high temperatures, R_\square can be fitted well with the thermally activated flux flow (TAFF) equation $R_\square = R_0 \exp(-U(B)/k_B T)$ [42] (shown by the dashed lines). Here, $U(B)$ is the thermal activation energy of the flux bundles (supplementary materials). However, at low temperatures, the data show pronounced deviations from the TAFF equation, and R_\square becomes independent of T . This phase is called the anomalous metal (AM) phase [22–27]. [Note that, in this context, the phases are defined by the value of the conductance σ as $T \rightarrow 0$: For a superconductor, $\sigma(T \rightarrow 0) = \infty$, for a metal $\sigma(T \rightarrow 0)$ is finite, and for an insulator $\sigma(T \rightarrow 0) = 0$.] We speculate that the AM phase perhaps arises due to the hopping of electrons between the phase-locked rare regions. This will drastically change the dissipative environment around the rare regions, suppressing the QGP. A rigorous theoretical analysis is required to verify if this is indeed the case. However, it has to be noted that, for instance, in MoGe films, the influence of a dissipative bath is known to trigger an anomalous metal phase (see, for example, [28]).

Even though our interpretation of the destruction of the IRFP in terms of the smearing scenario is physically appealing, it is not without its drawbacks. For one, the exact functional form of the temperature-dependent divergence of the effective exponent combination $z\nu$ is unknown for the smeared transition. Secondly, the tail that develops in figure 2(a) could have a different physical underpinning than what we have discussed regarding the smearing scenario. However, one can argue that there should be a stronger divergence than that displayed, for instance, by the IRCP or any critical point. The argument is based on the fact that in a smeared transition scenario, the dynamics of the finite-sized rare region are entirely frozen, thereby implying an infinite (at zero temperature) correlation time even when the correlation length is finite. In contrast, for any other transition (including IRCP) the correlation time only diverges concomitantly with the correlation length. This thus suggests a more substantial temperature-dependent divergence for the effective $z\nu$ combination than, for instance, the IRFP equation (3).

To rule out inadequate cooling of the electrons at ultra-low temperatures as the origin of the T -independence of R_{\square} , we measured the differential resistance as a function of DC current for different values of B for $V_g = 100$ V and at a fixed temperature $T = 20$ mK (figure 3(d)). The q-2DEG undergoes the superconducting to normal state transition as the current across it is increased beyond the critical current $I_c = 0.15 \mu\text{A}$ for $B_{\perp} = 0$ T. Application of B -field drives the system from the superconducting phase ($dV/dI = 0$) to the anomalous metallic state characterized by a finite dV/dI independent of I_{dc} and then to a weakly insulating state (decreasing dV/dI with an increase in I_c). Observing a finite conductance state in these sets of measurements, where the superconducting to insulator transition is current-driven at a fixed temperature, implies that these effects are not due to temperature saturation effects. Additionally, to avoid local heating of the vortex solid by high-frequency external radiation (which can lead to a low-temperature dissipative state [43]), each electrical line entering the dilution refrigerator was fitted with a three-stage low-pass cryogenic π filter with a cut-off frequency of 10 KHz (supplementary information, section S8) [44]. These measures give us the confidence that T -independence of R_{\square} is not an experimental artifact. The data on LAO/STO measured under identical conditions shows that such a resistance saturation is manifestly absent; this also rules out experimental artifacts as the origin of the resistance saturation in LAO/STO. This distinction between the low-temperature behavior of LSO/STO and LAO/STO heterostructures may be rooted in the amount of disorder in the two systems; the low- T resistance of LAO/STO is several times smaller than that of LSO/STO (figures 3(a) and (b)). We leave this question to future studies.

Quantum Griffiths effects are also expected to be cut off if the damping strength of a superconducting rare region grows less than its area. A large rare region has a well-developed superconducting gap [45–49]. Soft fermionic degrees of freedom can penetrate the rare region only up to a distance of the order of the coherence length. Thus, the damping strength for the largest rare regions can, at most, grow as their circumference rather than their area, destroying the Griffiths singularities below a characteristic temperature [24]. However, this mechanism would imply a crossover to a more conventional scenario, characterized by a finite value of the exponent νz in the low-temperature limit and conventional power-law scaling. This is not compatible with the experimental data presented in this letter.

In figure 3(e), we present the phase diagram for the system at $V_g = 100$ V constructed by combining the results obtained in the previous parts of this letter. It hosts several distinct phases and regimes not seen in previous studies on 2D superconductors [44]. At $T \rightarrow 0$, the superconducting phase (orange-shaded region; defined via the temperature where R_{\square} reaches 1% of its normal state value) and the conventional weakly localized normal state are separated by the possibly AM regime (green-shaded region). With increasing field (still at low temperatures), the system remains an AM while displaying the temperature-dependent cut-off of the Griffiths phase, wherein the putative Griffiths singularity gets cut off at low temperatures. With increasing temperature, the AM crosses over into a regime dominated by the thermally-assisted motion of vortices (pink-shaded region). The crossover between the AM and the TAFF regime (open blue squares) is defined as the points where R_{\square} deviates from the TAFF equation; see figure 3(a). Upon a further temperature increase, the system crosses over to a regime dominated by thermal fluctuations of the order parameter amplitude (blue-shaded region). This crossover line (marked by yellow stars) follows from a Ullah-Dorsey scaling analysis [50], as described in the supplemental materials. Finally, the crossover from the thermal fluctuation-dominated phase to the conventional weakly localized metal is reached at even higher temperatures. This crossover boundary (depicted by the purple triangles) is constructed following the discussion centered around figure 2(a).

1. Conclusions

To summarize, the superconductor-insulator transition in a q-2DEG formed at the interface of a LaScO₃/SrTiO₃ heterostructure displays an extremely unconventional critical behavior. The T -dependence of the critical exponent combination $z\nu(T)$ features two distinct regimes. At higher temperatures, the dependence of $z\nu(T)$ on both T and B follows the predictions of the IRCP scenario [13, 14, 35], and the sheet resistance data in this regime follow the predicted activated scaling law. In contrast, at lower temperatures, $z\nu$ has an unconventional power-law dependence on T . Such a power-law divergence not only disagrees with the IRCP scenario but is also inconsistent with a vanishing energy scale and, thus, with the very notion of a QCP. This implies that the putative Infinite Randomness superconducting critical point is destroyed, and consequently, the associated Griffith's behavior is suppressed below a temperature of about 0.07 K.

The physical mechanism leading to this low-temperature QGP suppression in LaScO₃/SrTiO₃ is not yet fully understood, including the nature of the subsequent ground state. It is also not clear what differentiates this heterostructure from its better-studied cousin LaAlO₃/SrTiO₃. It may be related to a change in the dissipative environment of the rare regions (i.e. superconducting puddles) caused by an interplay between long-range interactions and disorder [36, 37]. The low-temperature anomalies observed in figures 2(a)

and (c) can be thought to be consistent with the smearing scenario that is obtained from the combined effect of long-range interactions and disorder that leads to a change in the local dissipative environment. This, in turn, results in the freezing of the superconducting puddles, thus leading to a smearing of the IRCP and the cut-off of the Griffiths mechanism. However, as discussed before, the confirmation of this scenario is hampered by the fact that the functional form of the temperature-dependent divergence of the effective $z\nu$ combination is not known. However, physical arguments based on the freezing of dynamics for finite-size rare regions suggest a stronger divergence than that obtained for the case of the IRCP, consistent with our results.

We are thus led to a very important question on whether the cut-off of the Griffiths effects observed here is a material-specific phenomenon or whether it occurs generically at sufficiently low temperatures, effectively restricting the Griffiths singularities to an intermediate temperature regime. Answering this requires further theoretical and experimental studies.

Data availability statement

All data that support the findings of this study are included within the article (and any supplementary files).

Acknowledgments

A B acknowledges funding from the Science and Engineering Research Board, Govt. of India (No. HRR/2015/000017) and Department of Science and Technology, Govt. of India (No. DST/SJF/PSA01/2016-17). R N acknowledges funding from the Center for Quantum Information Theory in Matter and Spacetime, IIT Madras, and from the Department of Science and Technology, Govt. of India, under Grant No. DST/ICPS/QuST/Theme-3/2019/Q69, as well as support from the Mphasis F1 Foundation via the Centre for Quantum Information, Communication, and Computing (CQuICC). T V has been supported by the National Science Foundation under Grant No. DMR-1828489.

ORCID iDs

Anjana Dogra  <https://orcid.org/0000-0002-2678-4398>

Aveek Bid  <https://orcid.org/0000-0002-2378-7980>

References

- [1] Li W, Huang J, Li X, Zhao S, Lu J, Han Z V and Wang H 2021 *Mater. Today Phys.* **21** 100504
- [2] Brun C, Cren T and Roditchev D 2016 *Supercond. Sci. Technol.* **30** 013003
- [3] Wu Y *et al* 2021 *Phys. Rev. Lett.* **127** 180501
- [4] Wendum G 2017 *Rep. Prog. Phys.* **80** 106001
- [5] Wang H, Guo J, Miao J, Luo W, Gu Y, Xie R, Wang F, Zhang L, Wang P and Hu W 2022 *Small* **18** 2103963
- [6] Shi X, Lin P V, Sasagawa T, Dobrosavljevic V and Popovic D 2014 *Nat. Phys.* **10** 437
- [7] Xing Y *et al* 2015 *Science* **350** 542
- [8] Shen S *et al* 2016 *Phys. Rev. B* **94** 144517
- [9] Xing Y *et al* 2017 *Nano Lett.* **17** 6802
- [10] Saito Y, Nojima T and Iwasa Y 2018 *Nat. Commun.* **9** 1
- [11] Zhang C, Fan Y, Chen Q, Wang T, Liu X, Li Q, Yin Y and Li X 2019 *NPG Asia Mater.* **11** 1
- [12] Lewellyn N A, Percher I M, Nelson J, Garcia-Barriocanal J, Volotsenko I, Frydman A, Vojta T and Goldman A M 2019 *Phys. Rev. B* **99** 054515
- [13] Hoyos J A, Kotabage C and Vojta T 2007 *Phys. Rev. Lett.* **99** 230601
- [14] Vojta T, Kotabage C and Hoyos J A 2009 *Phys. Rev. B* **79** 024401
- [15] Ubaid-Kassis S, Vojta T and Schroeder A 2010 *Phys. Rev. Lett.* **104** 066402
- [16] Wang R *et al* 2017 *Phys. Rev. Lett.* **118** 267202
- [17] Reiss P, Graf D, Haghaghirad A A, Vojta T and Coldea A I 2021 *Phys. Rev. Lett.* **127** 246402
- [18] Fisher D S 1992 *Phys. Rev. Lett.* **69** 534
- [19] Vojta T 2006 *J. Phys. A: Math. Gen.* **39** R143
- [20] Vojta T 2013 *AIP Conf. Proc.* **1550** 188
- [21] Vojta T 2019 *Annu. Rev. Condens. Mater. Phys.* **10** 233
- [22] Abrahams E, Anderson P W, Licciardello D C and Ramakrishnan T V 1979 *Phys. Rev. Lett.* **42** 673
- [23] Chakravarty S, Yin L and Abrahams E 1998 *Phys. Rev. B* **58** R559
- [24] Kapitulnik A, Kivelson S A and Spivak B 2019 *Rev. Mod. Phys.* **91** 011002
- [25] Liu Y *et al* 2020 *Nano Lett.* **20** 5728
- [26] Li L, Chen C, Watanabe K, Taniguchi T, Zheng Y, Xu Z, Pereira V M, Loh K P and Castro Neto A H 2019 *Nano Lett.* **19** 4126
- [27] Saito Y, Kasahara Y, Ye J, Iwasa Y and Nojima T 2015 *Science* **350** 409
- [28] Mason N and Kapitulnik A 1999 *Phys. Rev. Lett.* **82** 5341
- [29] Kumar S, Kaswan J, Satpati B, Shukla A K, Gahtori B, Pulikkotil J J and Dogra A 2020 *Appl. Phys. Lett.* **116** 051603
- [30] Daptary G N, Kumar S, Bid A, Kumar P, Dogra A, Budhani R C, Kumar D, Mohanta N and Taraphder A 2017 *Phys. Rev. B* **95** 174502

- [31] Zeng S W, et al 2015 *Phys. Rev. B* **92** 020503
- [32] Liao M, Zhu Y, Zhang J, Zhong R, Schneeloch J, Gu G, Jiang K, Zhang D, Ma X and Xue Q-K 2018 *Nano Lett.* **18** 5660
- [33] Vojta T, Farquhar A and Mast J 2009 *Phys. Rev. E* **79** 011111
- [34] Fisher M P 1990 *Phys. Rev. Lett.* **65** 923
- [35] Del Maestro A, Rosenow B, Hoyos J A and Vojta T 2010 *Phys. Rev. Lett.* **105** 145702
- [36] Dobrosavljević V and Miranda E 2005 *Phys. Rev. Lett.* **94** 187203
- [37] Vojta T and Schmalian J 2005 *Phys. Rev. B* **72** 045438
- [38] Maiti S and Chubukov A V 2013 *AIP Conf. Proc.* **1550** 3
- [39] Vojta T 2003 *Phys. Rev. Lett.* **90** 107202
- [40] Hoyos J A and Vojta T 2008 *Phys. Rev. Lett.* **100** 240601
- [41] Hoyos J A and Vojta T 2012 *Phys. Rev. B* **85** 174403
- [42] Blatter G, Feigel'man M V, Geshkenbein V B, Larkin A I and Vinokur V M 1994 *Rev. Mod. Phys.* **66** 1125
- [43] Tamir I et al 2019 *Sci. Adv.* **5** eaau3826
- [44] Xing Y et al 2021 *Nano Lett.* **21** 7486
- [45] Karim Bouadim M R, Loh Y L and Trivedi N 2011 *Nat. Phys.* **7** 884
- [46] Tarat S and Majumdar P 2014 *Europhys. Lett.* **105** 67002
- [47] Swanson M, Loh Y L, Randeria M and Trivedi N 2014 *Phys. Rev. X* **4** 021007
- [48] Dubi Y, Meir Y and Avishai Y 2007 *Nature* **449** 876
- [49] Ghosal A, Randeria M and Trivedi N 2001 *Phys. Rev. B* **65** 014501
- [50] Ullah S and Dorsey A T 1991 *Phys. Rev. B* **44** 262